Construction of different dimensional inorganic–organic hybrid materials based on polyoxometalates and metal–organic units *via* changing metal ions: from non-covalent interactions to covalent connections†

Ya-Qian Lan, Shun-Li Li, Kui-Zhan Shao, Xin-Long Wang and Zhong-Min Su*

Received 15th February 2008, Accepted 9th May 2008
First published as an Advance Article on the web 13th June 2008
DOI: 10.1039/b802626b

Five POM-based hybrid materials have been designed and synthesized based on different metal ions under hydrothermal conditions, namely, $[Zn(Hfcz)(H_2O)_3](H_3fcz)(SiMo_{12}O_{40})\cdot 3H_2O$ (**1**), $[Cd_2(Hfcz)_6(H_2O)_2](SiMo_{12}O_{40})\cdot H_2O$ (**2**), $[Co_2(Hfcz)_2(SiW_{12}O_{40})](H_3fcz)_2(SiW_{12}O_{40})\cdot 10H_2O$ (**3**), $[Ni_2(Hfcz)_4(H_2O)_2](SiW_{12}O_{40})\cdot 5H_2O$ (**4**) and $[Ag_4(Hfcz)_2(SiMo_{12}O_{40})]$ (**5**), where Hfcz is fluconazole [2-(2,4-difluorophenyl)-1,3-di(1*H*-1,2,4-triazol-1-yl)propan-2-ol]. Their crystal structures have been determined by X-ray diffraction, elemental analyses, IR spectra, and thermogravimetric analyses (TGA). There are 1D mono and double chain-like metal–organic units in compounds **1** and **2**, respectively. Polyoxometalates and metal–organic units co-crystallize through hydrogen bonds. In compound **3**, metal–organic sheets are pillared by one kind of polyanion through covalent connections to generate a sandwich double-sheet. The other kind of polyanion acts as a counter-ion and lies in two adjacent sandwich double-sheets through non-covalent interactions. Polyanions covalently link metal–organic sheets to extend to an unusual 3D 5-connected framework with the $(4^4\cdot 6^6)$ topology in **4**. In compound **5**, polyanions link metal–organic chains to form a sheet through covalent connections. It is interesting that compound **5** shows an intricate (4,5,10)-connected framework with $(4^4\cdot 6^2)_4(4^8\cdot 6^2)_2(4^{14}\cdot 6^{19}\cdot 8^{12})$ topology based on two kinds of Ag cations as four-connected and five-connected nodes, and polyanions as ten-connected nodes, when Ag···O interactions are considered. It represents the highest connected network topology presently known for polyoxometalate systems. The structural differences among **1–5** indicate the importance of different metal–organic units, coordination modes of polyanions for framework formation, and the interactions between polyanions and metal–organic units. In addition, the luminescent properties of compounds **1**, **2** and **5**, and electrochemical behaviours of compounds **1–5** have been investigated.

Introduction

Polyoxometalates (POMs),[1] as a unique class of metal–oxide clusters, have many properties that make them attractive for applications in catalysis, medicine and materials science.[2] Several strategies have been considered to modify POMs while retaining their structural integrity, their intrinsic properties, and facilitating their implementation into extended structures. One common approach is the combination of the POMs and organic components resulting in the formation of POM-based inorganic–organic hybrid materials. To date, many POM-based hybrid materials have been obtained. Most of them are linked through non-covalent interactions[3] (van der Waals contacts, hydrogen bonding and/or ionic interactions) between the POMs and organic components. Covalent POM-based hybrid materials, compared with the above-mentioned hybrids, offer several advantages since covalent links improve the stability of the hybrid, might enhance the interaction between the inorganic and organic components and facilitate the construction of POM-based integrated nanosystems.[2a] However, only a few examples, such as covalently linked POMs and transition-metal complexes,[4] POM dendrimers,[5] POMs incorporated into polymers by copolymerization,[6] and conjugated polymer–POM hybrids,[7] have been observed.

Recently, with the rapid development of coordination polymers, a remarkable approach for constructing POM-based hybrid materials is the combination of POMs and transition-metal organic units.[8] The POMs, acting as unusual inorganic ligands, are introduced into the coordination polymers for the construction of various POM-based coordination polymers with desired properties.[9] This method incorporates two important research fields, namely coordination polymers and polyoxometalate chemistry, and opens up new possibilities in pursuit of multifunctional materials. Moreover, POM-based coordination polymers are prepared by hydrothermal reactions because of their poor solubility in water and in common organic solvents. This property is very advantageous in expanding the POM-based materials application in chemically bulk-modified electrodes.[10]

Institute of Functional Material Chemistry, Key Lab of Polyoxometalate Science of Ministry of Education, Faculty of Chemistry, Northeast Normal University, Changchun, 130024, China. E-mail: zmsu@nenu.edu.cn; Tel: +86 431 8509 9108

† Electronic supplementary information (ESI) available: Additional figures and TGA curves. CCDC reference numbers 678146 for **1**, 678143 for **2**, 678144 for **3**, 678145 for **4**, 678142 for **5**. For crystallographic data in CIF or other electronic format see DOI: 10.1039/b802626b

To date, many POM-based coordination polymers have been successfully assembled.[11] However, there is an unfavourable lack of investigation on the interactions (non-covalent interactions or covalent connections) between POM and metal–organic units. In comparison with other inorganic–organic coordination polymers, the rational design and assembly of POM-based coordination polymers, especially covalent connection, remains an arduous task for polyoxometalate chemists. To achieve this aim, several factors must be taken into account, such as the coordination geometry of the metal ions, the nature of the organic ligands, the use of a variety of POMs and the topological and geometrical relations between the metal ions and the ligand. Among these factors, the selection of the ligand is crucial. As a 1,2,4-triazole derivative, Hfcz (Hfcz is fluconazole (1-(2,4-difluorophenyl)-1,1-bis[(1*H*-1,2,4-triazol-1-yl)methyl]ethanol)) is not only a widely used antifungal medicine but is also a good flexible ligand to construct metal–organic polymers with optical properties and medical applications.[12] We and our co-workers have reported five novel compounds based on Hfcz ligands, the [β-Mo_8O_{26}]$^{4-}$ anions and different transition-metal ions.[12c] Furthermore, Keggin polyanions[13], as they are the most widely recognized and thoroughly studied among many different types of POMs, have widely been regarded as important molecular building units because they have a large number of terminal and bridging oxygen atoms that are potential coordination sites.[14] The research on the interactions between Keggin POMs and metal–organic units is significant.

Taking this into account, we chose Keggin polyanions [$SiR_{12}O_{40}$]$^{4-}$ (R = W and Mo), different metal ions and the Hfcz molecule, and five unique compounds have been obtained by hydrothermal methods, [Zn(Hfcz)(H_2O)$_3$](H_3fcz)($SiMo_{12}O_{40}$)·3H_2O (**1**), [Cd_2(Hfcz)$_6$(H_2O)$_2$]($SiMo_{12}O_{40}$)·H_2O (**2**), [Co_2(Hfcz)$_2$($SiW_{12}O_{40}$)](H_3fcz)$_2$($SiW_{12}O_{40}$)·10H_2O (**3**), [Ni_2(Hfcz)$_4$(H_2O)$_2$]($SiW_{12}O_{40}$)·5H_2O (**4**) and [Ag_4(Hfcz)$_2$($SiMo_{12}O_{40}$)] (**5**). The systematic investigation of the modulated effect of the various structural types of metal–organic units and coordination modes of Keggin polyanions on the ultimate framework will be represented and discussed. Changing metal ions not only obtains different dimensionalities of POM-based hybrid materials, but also influences the interactions (non-covalent interactions and/or covalent connections) between POMs and metal–organic units.

Experimental

General

All reagents and solvents for syntheses were purchased from commercial sources and used as received. The C, H, and N elemental analyses were conducted using a Perkin-Elmer 240C elemental analyzer. The FT-IR spectra were recorded as KBr pellets in the range 4000–400 cm^{-1} using a Mattson Alpha-Centauri spectrometer. Thermogravimetric analyses (TGA) of the samples were performed using a Perkin-Elmer TG-7 analyzer heated from room temperature to 1000 °C under nitrogen. Cyclic voltammograms (CV) were recorded using a 384B polarographic analyzer at room temperature (15–20 °C). A typical three-electrode cell having a CPE working electrode, a platinum counter electrode, and a silver/silver chloride reference electrode was used for the voltammetry experiments.

The **1**–**5**-modified carbon paste electrode **1**–CPE, **2**–CPE, **3**–CPE, **4**–CPE and **5**–CPE were fabricated according to the literature.[10e]

Syntheses of compounds

Synthesis of [Zn(Hfcz)(H_2O)$_3$](H_3fcz)($SiMo_{12}O_{40}$)·3H_2O (1). A mixture of $H_4SiMo_{12}O_{40}$ (0.24 g, 0.13 mmol), Hfcz (0.15 g, 0.5 mmol), $Zn(OAc)_2·2H_2O$ (0.029 g, 0.13 mmol) and H_2O (10 mL) was adjusted to pH ≈ 4–5, stirred for 1 h, and then transferred and sealed in a 25 mL Teflon-lined stainless-steel container that was heated at 150 °C for 72 h and then cooled to room temperature at a rate of 10 °C h^{-1}. Colorless crystals of **1** were collected in 68.9% yield based on $Zn(OAc)_2·2H_2O$. Elemental analyses calcd for $C_{26}H_{38}F_4Mo_{12}N_{12}O_{48}SiZn$ (2607.42): C 11.98; H 1.47; N 6.45. Found: C 12.00; H 1.45; N 6.49. IR (cm^{-1}): 3435 (w), 1697 (w), 1513 (w), 1425 (w), 1384 (w), 1054 (w), 999 (s), 874 (s), 793 (s), 592 (s).

Synthesis of [Cd_2(Hfcz)$_6$(H_2O)$_2$]($SiMo_{12}O_{40}$)·H_2O (2). Compound **2** was prepared similarly to compound **1** by using $Cd(OAc)_2·2H_2O$ (0.07 g, 0.26 mmol), instead of $Zn(OAc)_2·2H_2O$. Colorless crystals of **2** were obtained in 55.3% yield based on $Cd(OAc)_2·2H_2O$. Elemental analyses calcd for $C_{78}H_{78}Cd_2F_{12}Mo_{12}N_{36}O_{49}Si$ (3935.93): C 23.80; H 2.00; N 12.81. Found: C 23.82; H 1.99; N 12.79. IR (cm^{-1}): 3435 (w), 1644 (w), 1534 (w), 1430 (w), 1342 (m), 1098 (w), 943 (s), 838 (m), 796 (s), 587 (s).

Synthesis of [Co_2(Hfcz)$_2$($SiW_{12}O_{40}$)](H_3fcz)$_2$($SiW_{12}O_{40}$)·10H_2O (3). A mixture of $H_4SiW_{12}O_{40}$ (0.37 g, 0.13 mmol), Hfcz (0.15 g, 0.5 mmol), and $Co(OAc)_2·2H_2O$ (0.026 g, 0.13 mmol) in water (10 mL) was adjusted to pH ≈ 4–5, stirred for 1 h, and then transferred and sealed in a 25 mL Teflon-lined stainless-steel container that was heated at 150 °C for 72 h and then cooled to room temperature at a rate of 10 °C h^{-1}. Pink crystals of **3** were collected in 70.5% yield based on $Zn(OAc)_2·2H_2O$. Elemental analyses calcd for $C_{78}H_{100}Co_2F_{12}N_{36}O_{98}Si_2W_{24}$ (7924.38): C 11.82; H 1.27; N 6.36. Found: C 11.79; H 1.30; N 6.36. IR (cm^{-1}): 3436 (w), 3126 (m), 1621 (m), 1504 (s), 1425 (w), 1384 (w), 1282 (m), 1143 (m), 1017 (w), 970 (s), 888 (m), 797 (s), 648 (s), 512 (s).

Synthesis of [Ni_2(Hfcz)$_4$(H_2O)$_2$]($SiW_{12}O_{40}$)·5H_2O (4). Compound **4** was prepared similarly to compound **3** by using $NiCl_2·6H_2O$ (0.064 g, 0.26 mmol) instead of $Co(OAc)_2·2H_2O$. Green crystals of **4** were obtained in 75.3% yield based on $NiCl_2·6H_2O$. Elemental analyses calcd for $C_{52}H_{62}F_8N_{24}Ni_2O_{51}SiW_{12}$ (4342.97): C 14.38; H 1.44; N 7.74. Found: C 14.40; H 1.42; N 7.75. IR (cm^{-1}): 3437 (w), 3127 (m), 1625 (m), 1504 (s), 1415 (w), 1282 (m), 1130 (m), 970 (s), 927 (s), 887 (m), 796 (s), 675 (s), 512 (s).

Synthesis of [Ag_4(Hfcz)$_2$($SiMo_{12}O_{40}$)] (5). A mixture of $H_4SiMo_{12}O_{40}$ (0.24 g, 0.13 mmol), Hfcz (0.15 g, 0.5 mmol), $AgNO_3$ (0.022 g, 0.13 mmol), and H_2O (10 mL) was adjusted to pH ≈ 3, stirred for 1 h, and then transferred and sealed in a 25 mL Teflon-lined stainless-steel container. After the mixture was heated at 150 °C for 3 days, it was gradually cooled to room temperature at a rate of 10 °C h^{-1}. Colorless crystals of **5** were obtained. Yield: 49.5% based on $AgNO_3$. Elemental analyses calcd for $C_{26}H_{24}Ag_4F_4Mo_{12}N_{12}O_{42}Si$ (2863.42): C 10.91 H 0.84; N 5.87.

Found: C 10.89; H 0.85; N 5.88. IR (cm^{-1}): 3435 (w), 1614 (m), 1518 (s), 1499 (w), 1384 (s), 1054 (m), 956 (s), 863 (s), 793 (s), 592 (s), 505 (s).

X-Ray crystallography

Single-crystal X-ray diffraction data for compounds **1–5** were recorded using a Bruker Apex CCD diffractometer with graphite-monochromated MoK_α radiation ($\lambda = 0.71073$ Å) at 293 K. Absorption corrections were applied using a multi-scan technique. All the structures were solved by direct method of SHELXS-97[15] and refined by full-matrix least-squares techniques using the SHELXL-97 program[16] within WINGX.[17] Non-hydrogen atoms of complexes **1–5** were refined with anisotropic temperature parameters. Some C and O atoms of complexes **2–4** (C15, O1, O4, and O2W for **2**; O5W–O8W, O19, O19′ O20, O20′ O39, O39′ O40 and O40′ for **3**; O2W–O5W for **4**) were refined with isotropic temperature parameters and other non-hydrogen atoms were refined anisotropically. The disordered terminal O atoms of the polyanions in compounds **2–4**, the disordered O atoms of the water molecules in compound **1** (O5W, O5W′), and the disordered Cd2 atom **2** were refined using Cd and O atoms split over two sites, with a total occupancy of 1. The disordered heavy atoms were refined using W (W8 and W10) for **3** and W (W6) for **4**, atoms split over two sites, with a total occupancy of 1. The W1 atom in **4** was refined while being split over three sites, with a total occupancy of 1. For compounds **1–5**, the hydrogen atoms of the organic ligands were refined as rigid groups. All hydrogen atoms of the water molecules (O1W and O2W in **1**) were located from difference Fourier maps. Other water H atoms in compounds **1–4** could not be positioned reliably. The detailed crystallographic data and structure refinement parameters are summarized in Table 1.

Results and discussion

Syntheses of the compounds

Many POM-based coordination polymers with diverse structural architectures have been synthesized using hydrothermal methods. In most cases, the reaction mechanisms remain elusive and the control and prediction of crystal structures is very difficult, because the architecture of the final product depends directly on the interplay of starting materials, pH value, template, reaction temperature and pressure. In this case, the reaction pH value has an influence on the structural control of the self-assembly process. Compounds **1**, **2**, **3** and **4** have been isolated at pH ≈ 4–5, and pH ≈ 3 for **5**. In addition, we performed many experiments with similar synthetic conditions but with different pH values and compounds **1–5** could not be obtained. Therefore, the pH values have been adjusted to the conditions required to obtain the products.

Description of the structure

Single-crystal X-ray structural analysis reveals that the structure of **1** contains three kinds of units: polymeric chains $[Zn(Hfcz)(H_2O)_3]^{2+}$, protonated $(H_3fcz)^{2+}$ ligands and polyanions $(SiMo_{12}O_{40})^{4-}$. In the asymmetric unit, there is one Zn(II) cation, two Hfcz (Hfcz1 and Hfcz2) ligands, and one $(SiMo_{12}O_{40})^{4-}$ anion. In this case, the structure of the well known Keggin core is unexceptional, consisting of a central $\{SiO_4\}$ tetrahedron

Table 1 Crystal data and structure refinements for compounds **1–5**

	1	2	3	4	5
Formula	$C_{20}H_{38}F_4Mo_{12}N_{12}O_{48}SiZn$	$C_{78}H_{78}Cd_2F_{12}Mo_{12}N_{36}O_{49}Si$	$C_{78}H_{100}Co_2F_{12}N_{36}O_{98}Si_2W_{24}$	$C_{52}H_{62}F_8N_{24}Ni_2O_{51}SiW_{12}$	$C_{26}H_{24}Ag_4F_4Mo_{12}N_{12}O_{42}Si$
Formula weight	2607.42	3935.93	7924.38	4342.97	2863.42
Crystal system	Monoclinic	Triclinic	Monoclinic	Monoclinic	Triclinic
Space group	$P2_1/n$	$P\bar{1}$	$P2_1/c$	$P2_1/n$	$P\bar{1}$
a/Å	11.5540(4)	10.8680(17)	25.1472(10)	14.6355(4)	11.2237(6)
b/Å	23.1144(8)	16.260(3)	18.2073(7)	21.0669(5)	12.1149(7)
c/Å	23.6008(8)	17.493(3)	17.6380(7)	16.3476(8)	12.5214(7)
α/°	90	81.718(2)	90	90	61.840(1)
β/°	91.089(1)	79.092(3)	95.561(1)	98.291(1)	80.202(1)
γ/°	90	81.433(3)	90	90	73.756(1)
V/Å^3	6301.8(4)	2980.1(8)	8037.8(5)	4987.7(3)	1439.67(14)
Z	4	1	2	2	1
$D_{calc.}$/g cm^{-3}	2.748	2.193	3.274	2.892	3.303
$F(000)$	4984	1912	7140	3960	1342
Reflections collected/unique	38 270/14 847	16 955/12 756	48 729/18 599	30 037/11 838	7426/5049
R_{int}	0.0223	0.0346	0.0551	0.0743	0.0185
GOF on F^2	1.022	1.164	1.127	1.043	1.040
R_1[a] $[I>2\sigma(I)]$	0.0274	0.1329	0.0579	0.0503	0.0393
wR_2[b]	0.0647	0.2789	0.1123	0.1186	0.0851
Largest residuals/e Å^{-3}	1.363/−0.862	3.164/−2.281	2.330/−2.495	1.963/−3.749	1.224/−1.019

[a] $R_1 = \Sigma \| |F_o| - |F_c| \| / \Sigma |F_o|$. [b] $wR_2 = [\Sigma w(|F_o|^2 - |F_c|^2)] / \Sigma |w(F_o^2)^2|^{1/2}$.

surrounded by twelve $\{MO_6\}$ (M = Mo and W) octahedra arranged in four groups of three edge-sharing octahedral units, $\{M_3O_{13}\}$. Each of the trinuclear units is in turn linked by corner sharing to each other and to the central $\{SiO_4\}$ tetrahedron. As shown in Fig. 1a, the Zn(II) cation is coordinated by two nitrogen atoms [Zn(1)–N(4) = 1.976(3) Å and Zn(1)–N(3) = 1.999(3) Å] from different Hfcz molecules at the polar sites and three water molecules [Zn(1)–O(3 W) = 2.022(3) Å, Zn(1)–O(2 W) = 2.154(3) Å and Zn(1)–O(1 W) = 2.162(3) Å] at equatorial sites, showing a distorted trigonal bipyramidal coordination geometry [ZnN_2O_3]. The Zn–O and Zn–N bond lengths are all within the normal ranges.[18] Two kinds of Hfcz molecules show GT (G = *gauche* and T = *trans*) conformations with torsion angles of −40.8° and −169.9° for Hfcz1, and 56.6° and 176.1° for Hfcz2, respectively (Fig. S1, Table S1, ESI†). Each Hfcz1, acting as a bridging ligand, coordinates to two Zn(II) cations with two nitrogen atoms at the 4-position to generate a wave-like chain along the *a* axis (Fig. 1b). There are weak π···π stacking interactions between the 2,4-difluorophenyl ring and the imidazole ring in the same Hfcz ligand from the chain with the plane-to-plane distance of 3.40 Å and the centroid–centroid distance of 4.07 Å, which stabilizes the chain-like structure (Fig. S1c, ESI†). While each Hfcz2 molecule is protonated and accepts two H^+ ions. Each $(SiMo_{12}O_{40})^{4-}$ polyanion acts as a counter-ion.

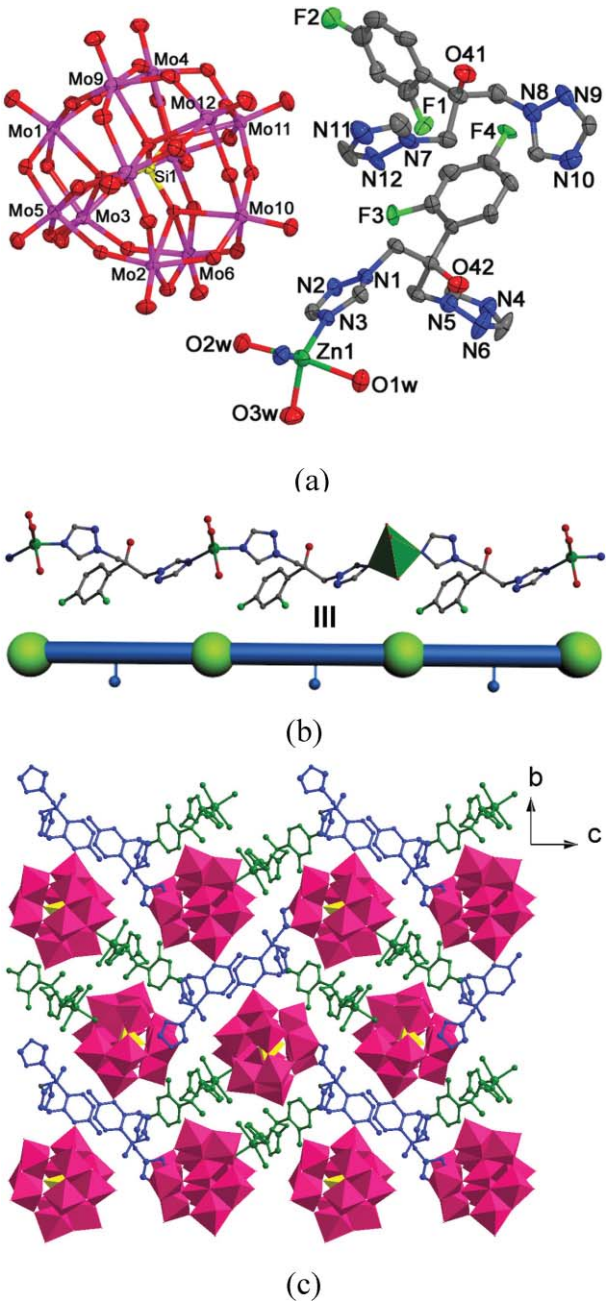

Fig. 1 (a) ORTEP plot of the asymmetric unit of compound **1**. (b) The 1D chain structure of **1**. (c) View of the arrangement of three types of isolated units in **1** (green and blue ball and stick representations of polymeric chains and protonated $(H_3fcz)^{2+}$ ligands, respectively).

It is interesting that coordination water molecules and OH^- groups from two kinds of Hfcz ligands donate H bonds to $(SiMo_{12}O_{40})^{4-}$ polyanions (Table S2, ESI†), which stabilizes the ultimate structure. $[Zn(Hfcz)(H_2O)_3]^{2+}$, $(H_3fcz)^{2+}$ and $(SiMo_{12}O_{40})^{4-}$ polyanions are closely packed to generate compound **1** through hydrogen bonds. (Fig. 1c).

Under similar reaction conditions, we obtained compound **2** by using Cd(II) ions instead of Zn(II) ions. In **2**, there exists two Cd ions, three Hfcz ligands and one $(SiMo_{12}O_{40})^{4-}$ anion. Each Cd(II) ion is six-coordinated by four nitrogen atoms from different Hfcz ligands and two water molecules for Cd1 [Cd(1)–N(18) = 2.293(15) Å, Cd(1)–N(12) = 2.402(15) Å and Cd(1)–O(1 W) = 2.365(15) Å], and six nitrogen atoms from different Hfcz ligands for Cd2 [Cd(2)–N(15) = 2.31(2) Å, Cd(2)–N(6) = 2.34(3) Å and Cd(2)–N(9) = 2.59(8) Å], respectively (Fig. 2a). They show octahedral coordination geometries [CdN_4O_2 and CdN_6]. The Cd–O and Cd–N distances are quite similar to the normal Cd–O and Cd–N distances.[19] Three kinds of Hfcz ligands show TT conformations with torsion angles of −171.4° and 171.4° for Hfcz1, −176.4° and 173.5° for Hfcz2, and 178.6° and 176.6° for Hfcz3, respectively (Fig. S2a–S2c, ESI†). Two kinds of Hfcz ligands link Cd1 and Cd2 ions to generate a hinge chain (Fig. 2b), and the other kind of Hfcz ligands as arms coordinated to Cd2 ions, which prevents the chain extending further. The chains with arms are paralleled and interlaced to form a pore that can accommodate the polyanions. In addition, each OH group of Hfcz from the arm donates a hydrogen bond to one bridging oxygen atom, which stabilizes the final structure (Table S2, ESI†). The arrangement of two kinds of compositions, chains and polyanions, are shown in Fig. 2c and Fig. S2d, ESI†.

Moreover, a 2D supramolecular network is finally formed by linking these chains through the weak π···π stacking interactions between 2,4-difluorophenyl rings and imidazole rings from adjacent chains, with the plane-to-plane distance of 3.46 Å and the centroid–centroid distance of 4.01 Å (Fig. S2e, ESI†).

Because Zn(II) and Cd(II) ions have a closed d^{10} electronic shell, there are no crystal-field stabilization energies for them when their complexes are formed. The coordination numbers of Zn(II) and Cd(II) ions are mainly determined by the steric repulsion between different ligands. Since the radius of a Cd(II) cation is larger than that of a Zn(II) cation, the coordination numbers of the Cd(II) cations in **2** are larger than those of the Zn(II) cations in **1**, which is similar to the reported results.[20] In **2**, each Cd(II) cation is coordinated by four or six Hfcz ligands, while each Zn(II) cation is linked by two Hfcz ligands. Therefore, compounds **1** and **2** show different chain-like structures.

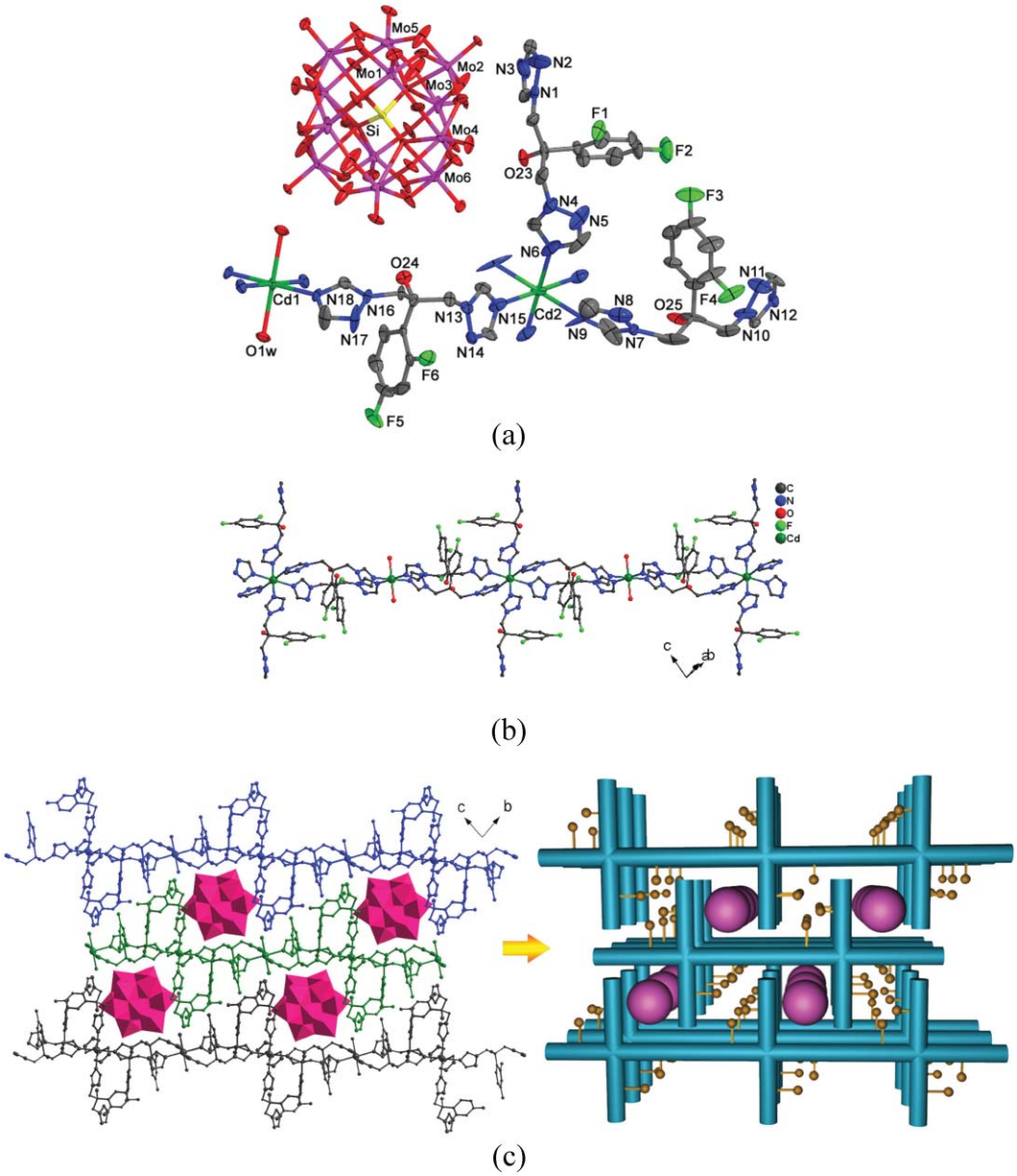

Fig. 2 (a) Coordination environment of the Cd(II) centers in compound **2** (all of the hydrogen atoms are omitted for clarity). (b) View of a hinge-chain structure. (c) Ball–stick and polyhedral and schematic representations of the arrangement of the two types of isolated units in **2**.

In order to investigate the influence of the metal center on the ultimate structure, Co(II) ions were selected and compound **3** has been isolated. There exists one kind of Co(II) ion, three kinds of Hfcz ligands and two kinds of $(SiW_{12}O_{40})^{4-}$ polyanions. As shown in Fig. 3a, each Co(II) ion is six-coordinated by four nitrogen atoms from different Hfcz ligands [Co(1)–N(9) = 2.090(10) Å, Co(1)–N(6) = 2.093(10) Å, Co(1)–N(10) = 2.101(10) Å and Co(1)–N(1) = 2.103(11) Å], one water molecule [Co(1)–O(1w) = 2.073(10) Å] and one terminal oxygen atom from one $(SiW_{12}O_{40})^{4-}$ polyanion [Co(1)–O(1) = 2.184(8) Å], which are consistent with values reported in the literature[12c], and shows an octahedral geometry [CoN_4O_2]. All Hfcz ligands show TT conformations and the torsion angles are 172.1° and 170.4° for Hfcz1, −166.7° and 178.3° for Hfcz2, and −164.8° and 173.6° for Hfcz3, respectively (Fig. S3a–3c, ESI†). Among them, two kinds of Hfcz ligands coordinate to Co(II) ions with the bis(monodentate) bridging modes to generate a $(4^4{\cdot}6^2)$ sheet (Fig. 3b, left), and all Co(II) ions are located in the sheet. Similar to compound **1**, there are weak π···π stacking interactions between the 2,4-difluorophenyl ring and the imidazole ring in the same Hfcz ligand with the plane-to-plane distance of 3.30 Å and the centroid–centroid distance of 3.79 Å (Fig. S3d, ESI†). The other kind of ligand is protonated. One of the $(SiW_{12}O_{40})^{4-}$ polyanions links to two Co(II) ions from adjacent layers with two crystallographically related terminal oxygen atoms. Therefore, adjacent $(4^4{\cdot}6^2)$ sheets are pillared by $(SiW_{12}O_{40})^{4-}$ polyanions to form a sandwich double structure with a thickness of 14.0572 Å (Fig. S3e, ESI†). The other kind of $(SiW_{12}O_{40})^{4-}$ polyanion acts as a counter-ion, which is

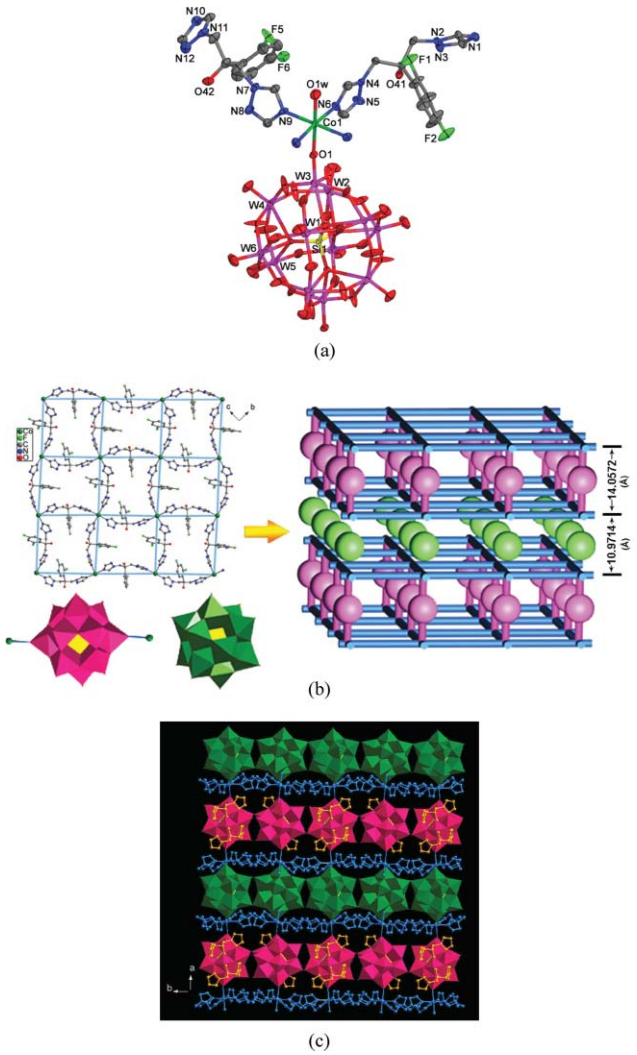

Fig. 3 (a) Coordination environment of the Co(II) center in compound **3** (all of the hydrogen atoms are omitted for clarity). (b) View of the structures of compound **3**. (c) Ball–stick and polyhedral representations of compound **3** [all 2,6-difluorophenyl (DFP) groups are omitted for clarity].

located between adjacent sandwich double sheets. The distance between two adjacent double sheets is 10.9714 Å, which is smaller than that in the double sheet (Fig. 3b, right, and Fig. S3f, ESI†). This may be caused by $(SiW_{12}O_{40})^{4-}$ polyanions. The $(SiW_{12}O_{40})^{4-}$ polyanions coordinating to metal centers can support metal–organic sheets, while dissociative $(SiW_{12}O_{40})^{4-}$ polyanions occupy the space between the sandwich double sheets.

Each protonated $(H_3fcz)^{2+}$ ligand donates one N–H $\cdots$ N bond to one Hfcz ligand and a O–H $\cdots$ O bond to a polyanion in the same sandwich double sheet (Table S1, ESI†), which makes all protonated $(H_3fcz)^{2+}$ ligands crystallize in the sheet. All dissociative polyanions are arranged between two sandwich double sheets (Fig. 3b, right, Fig. 3c and Fig. S3g, ESI†). Therefore, H-bonds play an important role in stabilizing the ultimate structure.

Different from **1** and **2**, Co(II) cations are connected by Hfcz ligands to form 2D metal–organic sheets, which are linked by one kind of polyanion through covalent connections to generate a sandwich double sheet. The other kind of polyanion acts as a counter-ion and lies in two adjacent sandwich double sheets through non-covalent interactions (Table S2, ESI†).

The above-mentioned results encouraged us to expand our studies to the Ni(II) analogues. The naive expectation was that the structural chemistry would be analogous to that of Co(II). In fact, while some analogies do exist, the results were largely unanticipated. X-Ray diffraction analysis reveals that compound **4** contains one kind of Ni(II) ion, two kinds of Hfcz ligands and one polyanion, when a Ni(II) ion is selected in the system. As shown in Fig. 4a, each Ni(II) ion shows an octahedral geometry $[NiN_4O_2]$, which is surrounded by four nitrogen atoms from different Hfcz ligands [Ni(1)–N(7) = 2.106(11) Å, Ni(1)–N(1) = 2.089(10) Å, Ni(1)–N(6) = 2.082(11) Å and Ni(1)–N(10) = 2.113(11) Å], one water molecule [Ni(1)–O(1W) = 2.095(10) Å] and one terminal oxygen from one polyanion [Ni(1)–O(22) = 2.155(9) Å], which are within the expected range.[12c] Two kinds of Hfcz ligands in GT conformations with torsion angles of 58.6° and 174.4° for Hfcz1, and 78.1° and 176.7° for Hfcz2, respectively (Fig. S4a–4b,

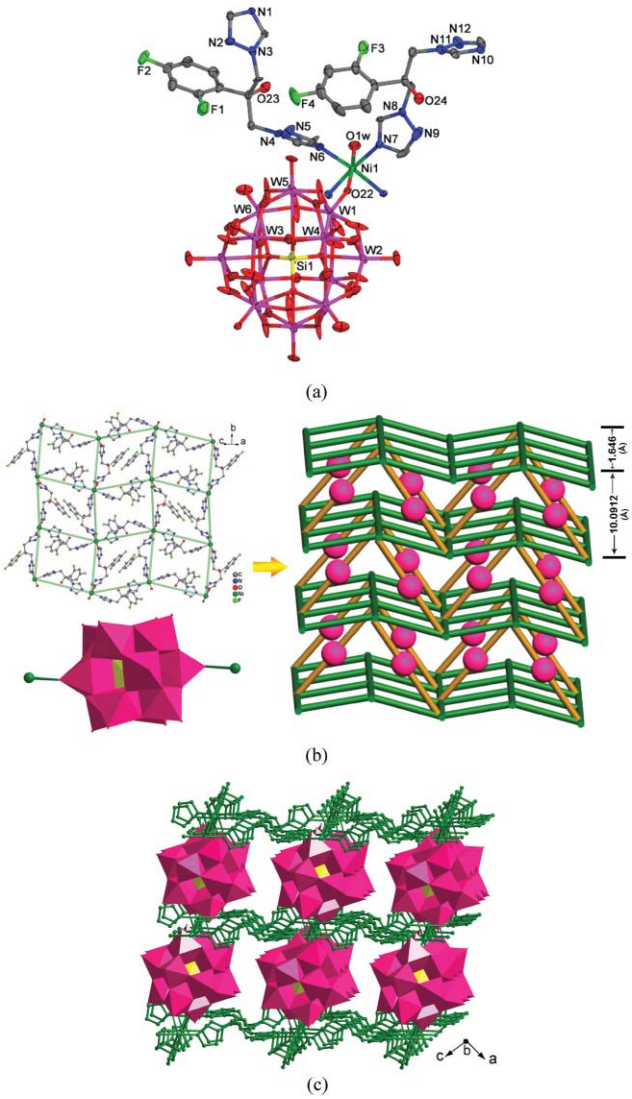

Fig. 4 (a) Coordination environment of the Ni(II) center in compound **4** (all of the hydrogen atoms are omitted for clarity). (b) View of the structures of compound **4**. (c) Ball–stick and polyhedral representations of compound **4** (all DFP groups are omitted for clarity).

ESI†), coordinate to two metal centers to generate a wave-like ($4^4 \cdot 6^2$) sheet (Fig. 4b, left) with a thickness of 1.646 Å (the thickness corresponding to both sides of the Ni(II) ions in the sheet) and there are weak $\pi \cdots \pi$ stacking interactions between the 2,4-difluorophenyl ring and the imidazole ring in the same Hfcz ligand with the plane-to-plane distance of 3.31 Å and the centroid–centroid distance of 3.84 Å (Fig. S4c, ESI†). Compared with compound **3**, this sheet is different from that in **3**. The sheet is plicated, polyanions can coordinate to Ni(II) ions from both sides of the sheet. The thickness of adjacent sheets is 10.0912 Å. Each polyanion links two Ni(II) ions from different sheets with crystallographically related terminal oxygen atoms to generate a 3D framework. From consideration of the Ni(II) ions as nodes and polyanions as linkers, we can see that the framework is comprised of a 5-connected ($4^4 \cdot 6^6$) topology (Fig. 4b right and Fig. 4c).

In compounds **3** and **4**, Co(II) and Ni(II) cations exhibit octahedral geometries ($[CoN_4O_2]$ and $[NiN_4O_2]$), which are linked by Hfcz ligands to generate different metal–organic ($4^4 \cdot 6^2$) sheets. Here, various coordination conformations (TT in **3** and GT in **4**) of the Hfcz ligands can result in changes in several aspects of the metal–organic units. For **3**, all Co(II) cations in the same sheet are planar, and all Ni(II) cations in the same sheet are located in two planes with a thickness of 1.646 Å in **4**. The wave-like sheets benefit from being coordinated by polyanions through covalent connections from both sides to generate a 3D framework in **4**.

To investigate the influence of metal centers on the complex frameworks, Ag(I) ions are selected to obtain compound **5**. For compound **5**, the asymmetric unit is composed of two kinds of Ag(I) ions, one kind of Hfcz ligand and polyanion (Fig. 5a). Ag1 cation is three-coordinated by two nitrogen atoms at the 4-position from different Hfcz ligands [Ag(1)–N(1) = 2.265(7) Å and Ag(1)–N(6) = 2.319(7) Å] and one terminal oxygen atom from the polyanion [Ag(1)–O(8) = 2.540(6) Å], and shows the T-shaped coordination geometry. Ag2 exhibits a closely linear coordination geometry, which is surrounded by two nitrogen atoms at the 2-position from different Hfcz ligands [Ag(2)–N(2) = 2.202(6) Å and Ag(2)–N(5) = 2.215(6) Å]. The Ag–O and Ag–N bond lengths are all within the expected ranges.[12c] The coordination mode of Hfcz ligand in **5** is different from **1–4**, which is coordinated to four Ag(I) cations with two nitrogen atoms at the 2-position and two nitrogen atoms at the 4-position, and shows TT conformation with torsion angles of −165.9° and −174.8° for Hfcz (Fig. S5a, ESI†). Two Hfcz ligands link two Ag2 cations with nitrogen atoms at the 2-position to form a unit of $(AgHfcz)_2^{2+}$, which contains of a 16-membered ring. These rings are extended to generate a chain by linking Ag1 cations with nitrogen atoms at the 4-position from Hfcz ligands (Fig. 5b). Each polyanion coordinates to two Ag1 cations with two terminal oxygen atoms. Therefore, compound **5** shows a 2D sheet (Fig. 5c).

In addition, each polyanion has $Ag \cdots O$ interactions with distances of 2.737 Å (Ag1–O8), 2.854 Å (Ag2–O17), 2.851 Å (Ag1–O10), 2.842 Å (Ag2–O4) and 2.836 Å (Ag2–O2). If these $Ag \cdots O$ non-covalent interactions are considered,[21] each polyanion can coordinate to ten Ag(I) cations to form an intricate 3D framework. From the topological view, if each Hfcz and Ag1 cation can be considered as four-connected nodes, respectively, Ag2 is considered as a five-connected node, and each polyanion is a ten-connected node (Fig. 5d), and the structure of **5** can be symbolized as an intricate (4,5,10)-connected framework with $(4^4 \cdot 6^2)_4(4^8 \cdot 6^2)_2(4^{14} \cdot 6^{19} \cdot 8^{12})$ topology (Fig. 5e). This represents the highest connected network topology presently known for polyoxometalate systems.

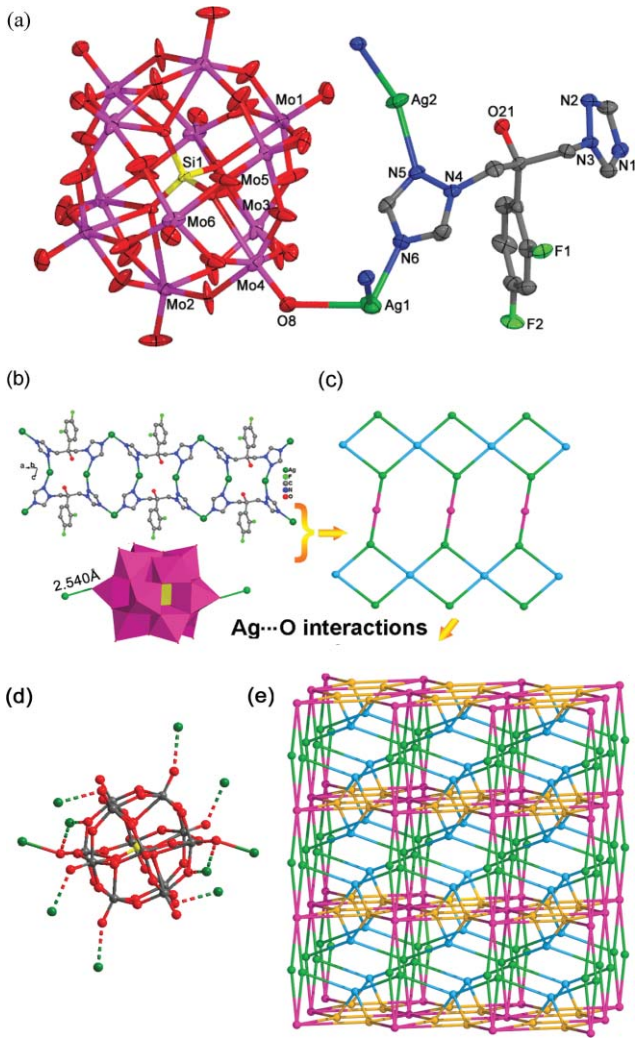

Fig. 5 (a) Coordination environment of the Ag(I) centers in compound **5** (all of the hydrogen atoms are omitted for clarity). (b) Ball–stick representation of Ag–Hfcz chain. (c) Ball–stick representation of the topological framework of **5** (blue, green and pink ball representations of three kinds of four-connected nodes for $(AgHfcz)_2^{2+}$ units, Ag1 cations and polyanions). (d) The coordination mode of the polyanion. (e) Ball–stick representation of the topological framework of **5** with $Ag \cdots O$ interactions (blue, green, yellow and pink ball representations of two kinds of four-connected nodes, five-connected nodes and ten-connected nodes for Hfcz, Ag1 cations, Ag2 cations and polyanions).

Metal–organic units on the molecular structures

According to previous research, the coordination ability of the nitrogen atoms from organic ligands is stronger than polyanions and water,[12c] therefore each metal cation is first coordinated by nitrogen atoms from Hfcz to generate different metal–organic units, which are further linked by polyanions to form the final products. In this case, the different coordination numbers and coordination geometries of Zn(II), Cd(II), Co(II), Ni(II) and Ag(I) cations are linked by Hfcz ligands with various coordination modes and conformations (TT and GT) to show multifarious

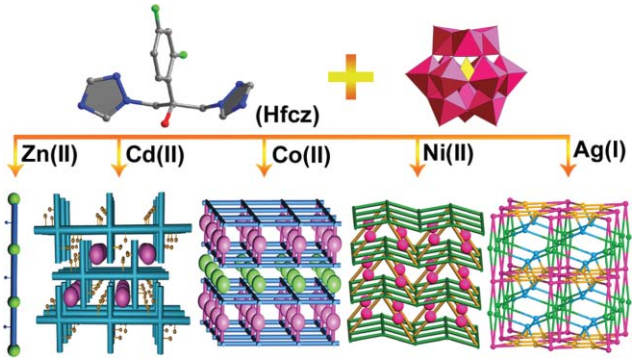

Scheme 1 Schematic view of the five compounds in this work.

metal–organic units. In **1**, **2** and **5**, Hfcz ligands connect Zn(II), Cd(II) and Ag(I) cations to form mono and double chains, respectively. While in **3** and **4**, Co(II) and Ni(II) cations are linked by Hfcz ligands with TT and GT conformations to extend to two kinds of $(4^4{\cdot}6^2)$ layers. These metal–organic units and polyanions are co-crystallized to form compounds **1–5**. Making a comparison to the above-mentioned structures of **1–5**, it can be seen that the metal–organic units have a great influence on the frameworks of the final compounds.

Coordination modes of Keggin-type polyanions

Further insight into the nature of the five compounds indicates that the coordination modes of Keggin-type polyanions have significant effects on the final structures of compounds **1–5**. The Keggin-type polyanions can coordinate to metal ions in a variety of coordination modes to form many attractive compounds with different dimensions.[22] In **1** and **2**, polyanions act as counter-ions and occupy the space that is formed by metal–organic unit packing. The polyanions play two roles in compound **3**. One of them acts as a bridge to link metal centers from different metal–organic sheets, and the other as a counter-ion to co-crystallize in the structure. In **4**, the polyanions are bidentate bridges linking the metal centers from different metal–organic units to form a 3D framework. In **5**, it is interesting that they connect covalently to two Ag(I) cations with two crystallographically related terminal oxygen atoms, and they have non-covalent interactions with the other eight Ag(I) cations and show ten-connected nodes. The intricate 3D topological framework of **5** may be due to the novel coordination mode of polyanions. From the structures of compounds **1–5**, it can be seen that the Keggin polyanions have a great influence on the frameworks of the complexes.

The interactions between POMs and metal–organic units

Based on the above-mentioned description, the interactions between POMs and metal–organic units play an important role in forming the ultimate structures. In **1** and **2**, different metal–organic chains and POMs are linked through hydrogen bonds. In **3**, metal–organic sheets are connected covalently by one kind of polyanion to form a sandwich double sheet. The other kind of polyanion co-crystallizes between adjacent sandwich double sheets through non-covalent interactions. While in **4**, the similar metal–organic sheets as in **3** are pillared by polyanions to generate a five-connected network through covalent connections. The polyanions covalently connect metal–organic chains to generate 2D sheets, which are linked by non-covalent Ag···O interactions to extend to the 3D framework in **5**.

These results indicate that different metal ions can form various metal–organic units. Different metal–organic units and polyanions with different coordination modes are linked to each other through non-covalent interactions and/or covalent connections to obtain different dimensionalities of POM-based hybrid materials.

Luminescent properties

Luminescent compounds are of great current interest because of their various applications in chemical sensors, photochemistry and electroluminescent (EL) displays.[23] The photoluminescent properties of compounds **1**, **2** and **5** were studied at room temperature (Fig. 6). It can be observed that the maximum emission wavelength occurs at 472 nm (λ_{ex} = 300 nm) for **1**, at 487 nm (λ_{ex} = 300 nm) for **2**, and 431 nm for **5** (λ_{ex} = 280 nm), which are red-shifted compared with that of pure Hfcz ligand (λ_{em} = 287 nm, λ_{ex} = 250 nm). The POMs ($H_4SiMo_{12}O_{40}$ and $H_4SiW_{12}O_{40}$) are nearly non-fluorescent in the range 200–700 nm for excitation wavelengths between 250 and 300 nm at ambient temperature. The emission of **1**, **2** and **5** may be assigned to a joint contribution of the intra-ligand transitions or charge-transfer transitions between the coordinated ligands and the metal center. In comparison with the free ligands, the emission maximums of compounds **1**, **2** and **5** have changed. This may be caused by the following: (1) after coordinating to metal centers, neutral ligands may change their HOMO and LUMO energy levels; (2) compounds **1**, **2** and **5** may have charge-transfer transitions between ligands and metal centers.

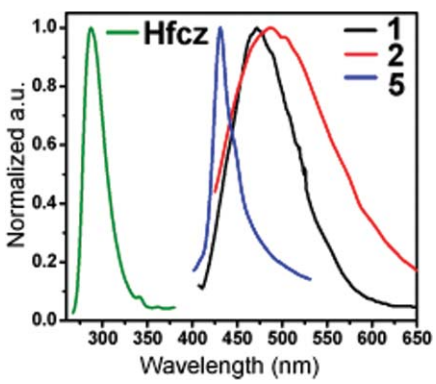

Fig. 6 Emission spectra of **1**, **2**, **5** and Hfcz in the solid state at room temperature.

Electrochemical behaviors of the 1–CPE, 2–CPE, 3–CPE, 4–CPE and 5–CPE

The electrochemical behaviours of **1**–CPE, **2**–CPE, **3**–CPE, **4**–CPE and **5**–CPE were studied. Fig. 7 shows the typical cyclic voltammograms at a potential range od −100–800 mV for **1**–CPE, **2**–CPE and **5**–CPE, at a potential range of −700–300 mV for **3**–CPE and **4**–CPE. It can be clearly seen that three reversible redox peaks appear in 1 M H_2SO_4 aqueous solution, respectively. Redox peaks I–I′, II–II′, and III–III′ correspond to three consecutive two-electron processes, respectively. The approximate proportionality

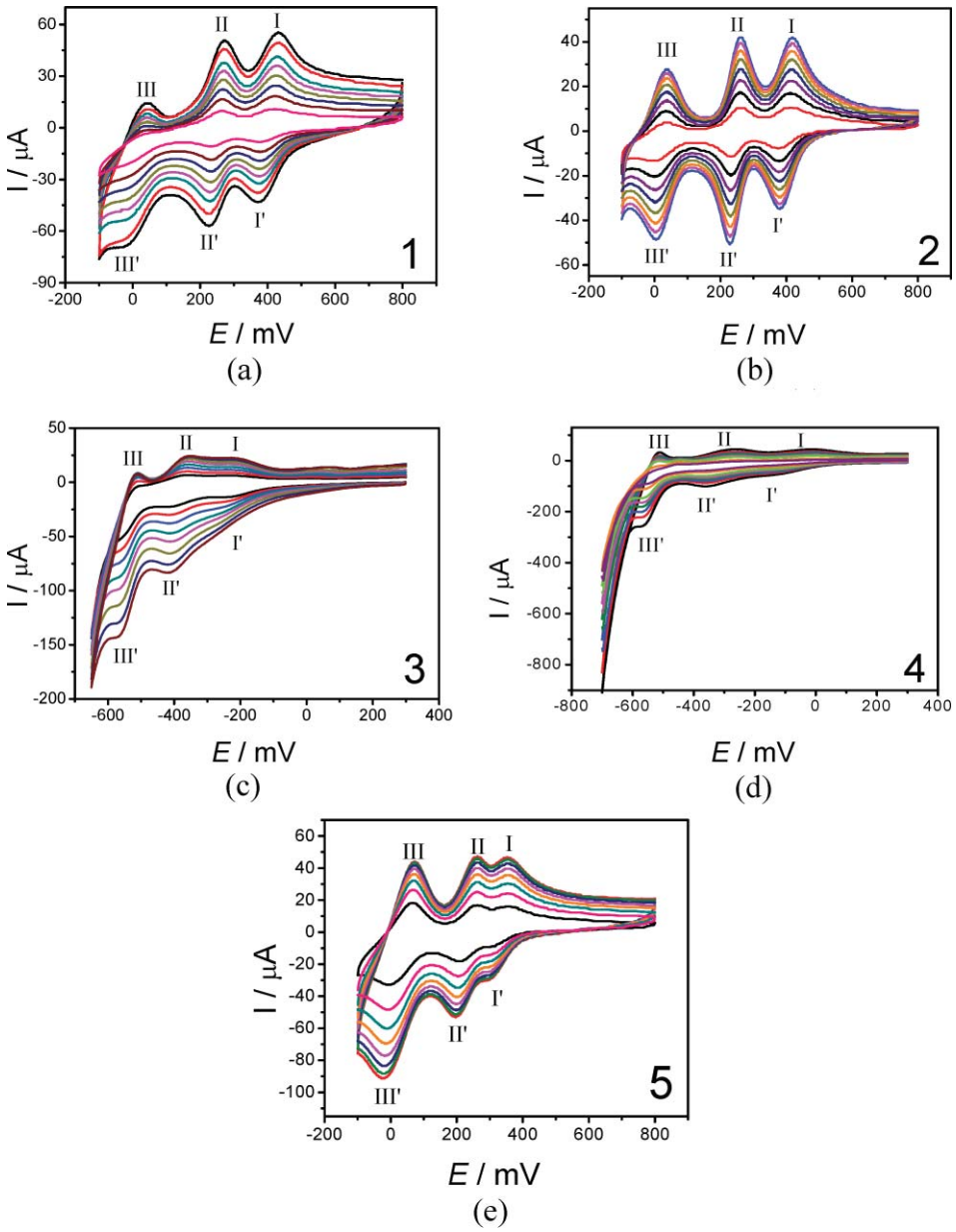

Fig. 7 The cyclic voltammograms of **1**–CPE (a), **2**–CPE (b), **3**–CPE (c), **4**–CPE (d) and **5**–CPE (e) in 1 M H_2SO_4 at different scan rates (from inner to outer: 50, 100, 150, 200, 250, 300, 350 and 400 mV s^{-1}).

of the reduction peak current to the scan rate up to 400 mV s^{-1} (Fig. 8) indicates that the redox process is surface-controlled for **1**–CPE, **3**–CPE and **4**–CPE. At scan rates lower than 100 mV s^{-1}, the peak currents are proportional to the scan rate, which indicates the redox process of **2**–CPE and **5**–CPE are surface-controlled; however, at scan rates higher than 150 mV s^{-1}, the peak currents are proportional to the square root of the scan rate, which indicates the redox process of **2**–CPE and **5**–CPE are diffusion-controlled.

As shown in Fig. 9, **1**–CPE, **2**–CPE and **5**–CPE display good electrocatalytic activity toward the reduction of nitrite in 1 M H_2SO_4 containing $NaNO_2$. Upon addition of NO_2^-, the reduction peak currents increase and the corresponding oxidation peak currents decrease dramatically, and this suggests that the nitrite is reduced.[24] These results indicate that the three reduced species all have electrocatalytic activity for nitrite reduction. It was also noted that the third reduced species showed the best electrocatalytic activity, that is, the catalytic activity is enhanced with increasing extent of the polyanion reduction.

Based on the above-mentioned investigation, we have found that compounds **1**, **2** and **5** show similar electrochemical behaviours, which are caused by $(SiMo_{12}O_{40})^{4-}$ anions. Compounds **3** and **4** exhibit similar electrochemical behaviours to those of $(SiW_{12}O_{40})^{4-}$ anions, and compounds based on $(SiMo_{12}O_{40})^{4-}$ anions display better electrocatalytic activities than those based on $(SiW_{12}O_{40})^{4-}$ anions.

Thermal analysis

In order to characterize the compounds more fully in terms of their thermal stability, we examined **1–5** using TGA. The experiment

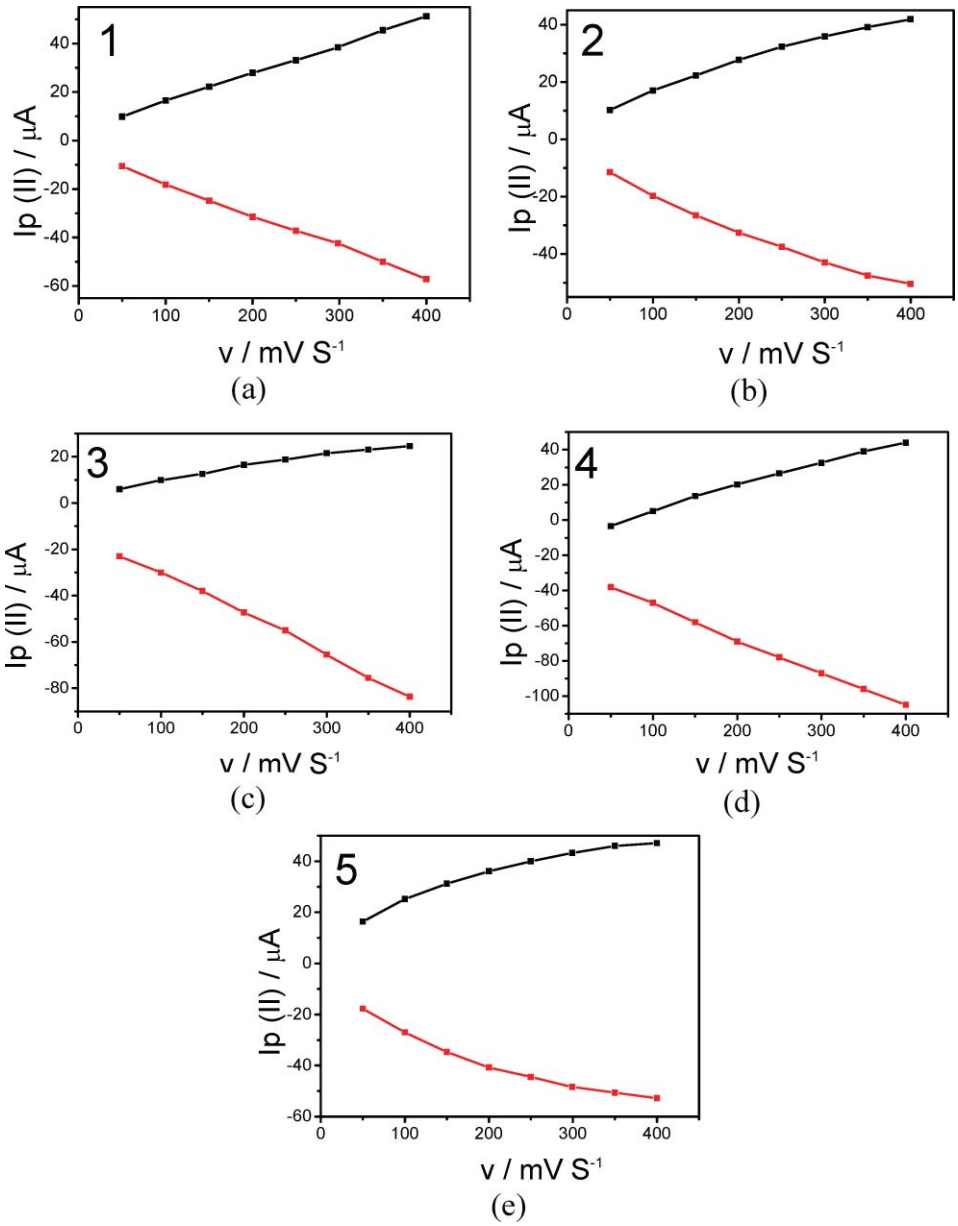

Fig. 8 The plots of the anodic and the cathodic peak II–II′ currents against scan rates for **1**–CPE (a), **2**–CPE (b), **3**–CPE (c), **4**–CPE (d) and **5**–CPE (e).

was performed on samples consisting of numerous single crystals of **1–5** under a N_2 atmosphere with a heating rate of 10 °C min^{-1} (Fig. S6, ESI†).

For compound **1**, the weight loss corresponding to the release of six water molecules is observed from room temperature to 165 °C (obsd 4.3%, calcd 4.15%). The destruction of the anhydrous compound occurs from 301 to 864 °C. The TGA curve of **2** shows that it undergoes dehydration in the temperature range of 15–120 °C. This corresponds to the loss of water molecules (obsd 1.6%, calcd 1.37%). From 334 to 894 °C, the anhydrous compound decomposes with a step-wise loss of the organic composition. Compound **3** lost its water molecules from room temperature to 45 °C (obsd 2.4%, calcd 2.27%). The anhydrous $[Co_2(Hfcz)_2(SiW_{12}O_{40})](H_3fcz)_2(SiW_{12}O_{40})$ is stable up to 211 °C, and the removal of organic components occurs from 211 to 842 °C. For compound **4**, the weight loss in the range of 20–131 °C corresponds to the loss of water molecules (obsd 3.0%, calcd 2.90%). The removal of the organic components occurs at 255 °C. The decomposition of the anhydrous compound **5** occurs at 232 °C.

Conclusion

In summary, five POM-based inorganic–organic hybrid materials based on fluconazole, various metal ions and Keggin polyanions have been synthesized by hydrothermal methods. The results indicate that different metal ions can form various metal–organic units and different metal–organic units, and polyanions with different coordination modes are linked to each other through non-covalent interactions and/or covalent connections to obtain different dimensionalities of compounds. In these systems, Co, Ni and Ag ions are favoured for the formation of compounds by covalent

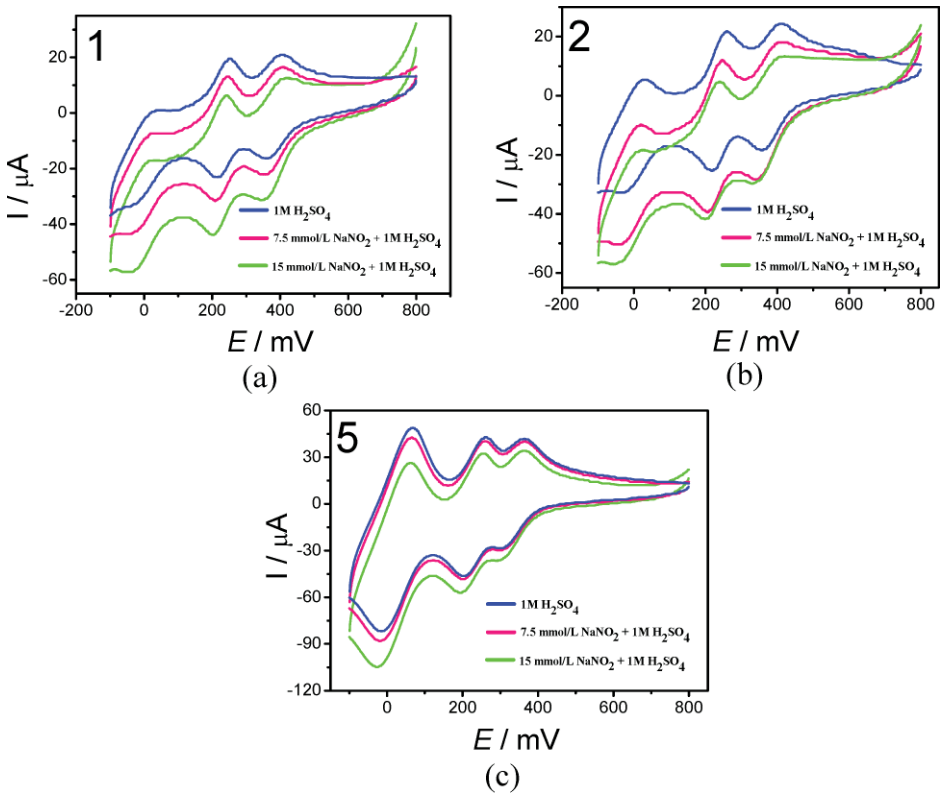

Fig. 9 Cyclic voltammograms of **1**–CPE (a), **2**–CPE (b) and **5**–CPE (c) in 1 M H_2SO_4 containing different concentrations of NO_2^-.

connections with polyanions than Zn and Cd ions. In addition, these compounds show interesting fluorescent and electrochemical properties. The successful isolation of these compounds not only provides intriguing examples of POM-based hybrid materials but may also open up possibilities for the design of new inorganic–organic hybrid materials with particular functions in the near future.

Acknowledgements

We are thankful for financial support from the Program for Changjiang Scholars and Innovative Research Team in University, The National Natural Science Foundation of China (No. 20 573 016 and 20 703 008), and the Science Foundation for Young Teachers of Northeast Normal University (No. 20 070 309).

References

1 (*a*) M. T. Pope, *Heteropoly and Isopoly Oxometalates*, Springer, Berlin, Germany, 1983; (*b*) C.-D. Wu, C.-Z. Lu, H.-H. Zhuang and J.-S. Huang, *J. Am. Chem. Soc.*, 2002, **124**, 3836; (*c*) C. L. Hill, *Chem. Rev.*, 1998, **98**, 1; (*d*) M. I. Khan, E. Yohannes and R. J. Doedens, *Angew. Chem., Int. Ed.*, 1999, **38**, 1292; (*e*) K. Fukaya and T. Yamase, *Angew. Chem., Int. Ed.*, 2003, **42**, 654; (*f*) E. Burkholder and J. Zubieta, *Chem. Commun.*, 2001, 2056; (*g*) P. J. Hagrman, D. Hagrman and J. Zubieta, *Angew. Chem., Int. Ed.*, 1999, **38**, 2638.

2 (*a*) T. Yamase, *Chem. Rev.*, 1998, **98**, 307; (*b*) A. Müller, S. Q. N. Shah, H. Bögge and M. Schmidtmann, *Nature*, 1999, **397**, 48; (*c*) L. Xu, M. Lu, B. Xu, Y. Wei, Z. Peng and D. R. Powell, *Angew. Chem., Int. Ed.*, 2002, **41**, 4129; (*d*) L. Chen, F. Jiang, Z. Lin, Y. Zhou, C. Yue and M. Hong, *J. Am. Chem. Soc.*, 2005, **127**, 8588; (*e*) P. Kögerler and L. Cronin, *Angew. Chem., Int. Ed.*, 2005, **44**, 844; (*f*) E. Coronado and C. J. Gómez-García, *Chem. Rev.*, 1998, **98**, 273; (*g*) P. Wang, X. Wang and G. Zhu, *New J. Chem.*, 2000, **24**, 481; (*h*) P. Wang, X. Wang and G. Zhu, *Electrochim. Acta*, 2000, **46**, 637.

3 (*a*) C. Sanchez and F. Ribot, *New J. Chem.*, 1994, **18**, 1007; (*b*) C. Sanchez, G. J. A. A. Soler-Illia, F. Ribot, T. Lalot, C. R. Mayer and V. Cabuil, *Chem. Mater.*, 2001, **13**, 3061; (*c*) S. Chakrabarti and S. Natarajan, *Cryst. Growth Des.*, 2002, **2**, 333; (*d*) T. R. Veltman, A. K. Stover, A. Narducci-Sarjeant, K. M. Ok, P. S. Halasyamani and A. J. Norquist, *Inorg. Chem.*, 2006, **45**, 5529; (*e*) R. Atencio, A. Briceño, P. Silva, J. A. Rodríguez and J. C. Hanson, *New J. Chem.*, 2007, **31**, 33.

4 (*a*) S. Favette, B. Hasenknopf, J. Vaissermann, P. Gouzerh and C. Roux, *Chem. Commun.*, 2003, 2664; (*b*) J. W. Han, K. I. Hardcastle and C. L. Hill, *Eur. J. Inorg. Chem.*, 2006, 2598; (*c*) J. Kang, B. Xu, Z. Peng, X. Zhu, Y. Wei and D. R. Powell, *Angew. Chem., Int. Ed.*, 2005, **44**, 6902; (*d*) K. Pavani and A. Ramanan, *Eur. J. Inorg. Chem.*, 2005, 3080; (*e*) L. Lisnard, A. Dolbecq, P. Mialane, J. Marrot, E. Codjovi and F. Sécheresse, *Dalton Trans.*, 2005, 3913; (*f*) H. Abbas, C. Streb, A. L. Pickering, A. R. Neil, D. Long and L. Cronin, *Cryst. Growth Des.*, 2008, **8**, 635; (*g*) K. Pavani, S. E. Lofland, K. V. Ramanujachary and A. Ramanan, *Eur. J. Inorg. Chem.*, 2007, 568; (*h*) R. C. Finn and J. Zubieta, *Inorg. Chem.*, 2001, **40**, 2466; (*i*) R. C. Finn, R. S. Rarig and J. Zubieta, *Inorg. Chem.*, 2002, **41**, 2109; (*j*) E. Burkholder, S. Wright, V. Golub, C. J. O'Connor and J. Zubieta, *Inorg. Chem.*, 2003, **42**, 7460; (*k*) E. Burkholder, V. Golub, C. J. O'Connor and J. Zubieta, *Inorg. Chem.*, 2003, **42**, 6729; (*l*) E. Burkholder, V. Golub, C. J. O'Connor and J. Zubieta, *Inorg. Chem.*, 2004, **43**, 7014.

5 (*a*) H. Zeng, G. R. Newkome and C. L. Hill, *Angew. Chem., Int. Ed.*, 2000, **39**, 1771; (*b*) J. R. Morgan and M. J. Cloninger, *J. Polym. Sci., Part A: Polym. Chem.*, 2005, **43**, 3059.

6 (*a*) P. Judeinstein, *Chem. Mater.*, 1992, **4**, 4; (*b*) C. R. Mayer, V. Cabuil, T. Lalot and R. Thouvenot, *Angew. Chem., Int. Ed.*, 1999, **38**, 3672; (*c*) C. R. Mayer, R. Thouvenot and T. Lalot, *Chem. Mater.*, 2000, **12**, 257; (*d*) C. R. Mayer, R. Thouvenot and T. Lalot, *Macromolecules*, 2000, **33**, 4433; (*e*) A. R. Moore, H. Kwen, A. M. Beatty and E. A. Maatta, *Chem. Commun.*, 2000, 1793.

7 (*a*) M. Lu, B. Xie, J. Kang, F.-C. Chen, Y. Yang and Z. Peng, *Chem. Mater.*, 2005, **17**, 402; (*b*) B. Xu, M. Lu, J. Kang, D. Wang, J. Brown and Z. Peng, *Chem. Mater.*, 2005, **17**, 2841.

8 (*a*) D. Hagrman, P. J. Hagrman and J. Zubieta, *Angew. Chem., Int. Ed.*, 1999, **38**, 3165; (*b*) D. Hagrman, C. Zubieta, D. J. Rose, J. Zubieta and R. C. Haushalter, *Angew. Chem., Int. Ed. Engl.*, 1997, **36**, 873; (*c*) C. Streb, C. Ritchie, D.-L. Long, P. Kögerler and L. Cronin, *Angew. Chem., Int. Ed.*, 2007, **46**, 7579; (*d*) C. Inman, J. M. Knaust and S. W. Keller, *Chem. Commun.*, 2002, 156.

9 (*a*) W.-M. Bu, L. Ye, G.-Y. Yang, J.-S. Gao, Y.-G. Fan, M.-C. Shao and J.-Q. Xu, *Inorg. Chem. Commun.*, 2001, **4**, 1; (*b*) C.-M. Liu, D.-Q. Zhang, C.-Y. Xu and D.-B. Zhu, *Solid State Sci.*, 2004, **6**, 689; (*c*) J. Chen, S. Lu, R. Yu, Z. Chen, Z. Huang and C. Lu, *Chem. Commun.*, 2002, 2640; (*d*) C.-D. Wu, C.-Z. Lu, X. Lin, H.-H. Zhuang and J.-S. Huang, *Inorg. Chem. Commun.*, 2002, **5**, 664; (*e*) C.-M. Liu, D.-Q. Zhang, M. Xiong and D.-B. Zhu, *Chem. Commun.*, 2002, 1416; (*f*) B.-Z. Lin and S.-X. Liu, *Chem. Commun.*, 2002, 2126; (*g*) S. Uchida and N. Mizuno, *J. Am. Chem. Soc.*, 2004, **126**, 1602; (*h*) X. M. Zhang, M. L. Tong, S. H. Feng and X. M. Chen, *J. Chem. Soc., Dalton Trans.*, 2001, 2069; (*i*) C.-Z. Lu, C.-D. Wu, H.-H. Zhuang and J.-S. Huang, *Chem. Mater.*, 2002, **14**, 2649; (*j*) L.-M. Zheng, Y. Wang, X. Wang, J. D. Korp and A. J. Jacobson, *Inorg. Chem.*, 2001, **40**, 1380; (*k*) R. Kawamoto, S. Uchida and N. Mizuno, *J. Am. Chem. Soc.*, 2005, **127**, 10560.

10 (*a*) K. Kalcber, *Electroanalysis*, 1990, **2**, 419; (*b*) X.-L. Wang, E.-B. Wang, Y. Lan and C.-W. Hu, *Electroanalysis*, 2002, **14**, 1116; (*c*) X.-L. Wang, C. Qin, E.-B. Wang, Z.-M. Su, Y.-G. Li and L. Xu, *Angew. Chem., Int. Ed.*, 2006, **45**, 7411; (*d*) X. Wang, E. Wang and C. Hu, *Chem. Lett.*, 2001, 1030; (*e*) Z. Han, Y. Zhao, J. Peng, Q. Liu and E. Wang, *Electrochim. Acta*, 2005, **51**, 218; (*f*) Z. Han, Y. Zhao, J. Peng, A. Tian, Y. Feng and Q. Liu, *Electrochim. Acta*, 2005, **178**, 1386.

11 (*a*) Y. P. Jeannin, *Chem. Rev.*, 1998, **98**, 51; (*b*) X.-B. Cui, J.-Q. Xu, H. Meng, S.-T. Zheng and G.-Y. Yang, *Inorg. Chem.*, 2004, **43**, 8005; (*c*) U. Kortz, M. G. Savelieff, F. Y. A. Ghali, L. M. Khalil, S. A. Maalouf and D. I. Sinno, *Angew. Chem., Int. Ed.*, 2002, **41**, 4070; (*d*) L. C. W. Baker and D. C. Glick, *Chem. Rev.*, 1998, **98**, 3; (*e*) A. Müller, F. Peters, M. T. Pope and D. Gatteschi, *Chem. Rev.*, 1998, **98**, 239; (*f*) P. Gouzerh and A. Proust, *Chem. Rev.*, 1998, **98**, 77; (*g*) E. Burkholder, V. Golub, C. J. O'Connor and J. Zubieta, *Chem. Commun.*, 2003, 2128; (*h*) R. C. Finn, E. Burkholder and J. Zubieta, *Chem. Commun.*, 2001, 1852; (*i*) M. T. Pope and A. Müller, *Angew. Chem., Int. Ed. Engl.*, 1991, **30**, 34; (*j*) U. Kortz, F. Hussain and M. Reicke, *Angew. Chem., Int. Ed.*, 2005, **44**, 3773; (*k*) H. An, Y. Li, E. Wang, D. Xiao, C. Sun and L. Xu, *Inorg. Chem.*, 2005, **44**, 6062; (*l*) J. Lu, E.-H. Shen, M. Yuan, Y.-G. Li, E.-B. Wang, C.-W. Hu, L. Xu and J. Peng, *Inorg. Chem.*, 2003, **42**, 6956.

12 (*a*) H. Han, Y. Song, H. Hou, Y. Fan and Y. Zhu, *Dalton Trans.*, 2006, 1972; (*b*) H. Han, S. Zhang, H. Hou, Y. Fan and Y. Zhu, *Eur. J. Inorg. Chem.*, 2006, 1594; (*c*) S.-L. Li, Y.-Q. Lan, J.-F. Ma, J. Yang, X.-H. Wang and Z.-M. Su, *Inorg. Chem.*, 2007, **46**, 8283.

13 J. F. Keggin, *Proc. R. Soc. London, Ser. A*, 1934, **144**, 75.

14 (*a*) X.-J. Kong, Y.-P. Ren, P.-Q. Zheng, Y.-X. Long, L.-S. Long, R.-B. Huang and L.-S. Zheng, *Inorg. Chem.*, 2006, **45**, 10702; (*b*) Y.-P. Ren, X.-J. Kong, X.-Y. Hu, M. Sun, L.-S. Long, R.-B. Huang and L.-S. Zheng, *Inorg. Chem.*, 2006, **45**, 4016; (*c*) P.-Q. Zheng, Y.-P. Ren, L.-S. Long, R.-B. Huang and L.-S. Zheng, *Inorg. Chem.*, 2005, **44**, 1190; (*d*) J. Lu, E. H. Shen, Y. G. Li, D. R. Xiao, E. B. Wang and L. Xu, *Cryst. Growth Des.*, 2005, **5**, 65.

15 G. M. Sheldrick, *SHELXS-97, Program for solution of crystal structures*, University of Göttingen, Germany, 1997.

16 G. M. Sheldrick, *SHELXL-97, Program for refinement of crystal structures*, University of Göttingen, Germany, 1997.

17 L. J. Farrugia, *WINGX, A Windows program for crystal structure analysis*, University of Glasgow, Glasgow, UK, 1988.

18 (*a*) W. Chen, H.-M. Yuan, J.-Y. Wang, Z.-Y. Liu, J.-J. Xu, M. Yang and J.-S. Chen, *J. Am. Chem. Soc.*, 2003, **125**, 9266; (*b*) A. Majumder, S. Shit, C. R. Choudhury, S. R. Batten, G. Pilet, D. Luneau, N. Daro, J.-P. Sutter, N. Chattopadhyay and S. Mitra, *Inorg. Chim. Acta*, 2005, **358**, 3855; (*c*) S. V. Ganesan and S. Natarajan, *Inorg. Chem.*, 2004, **43**, 198; (*d*) J.-P. Zhang, Y.-Y. Lin, X.-C. Huang and X.-M. Chen, *Eur. J. Inorg. Chem.*, 2006, 3407; (*e*) D. Sun, R. Cao, Y. Liang, Q. Shi, W. Su and M. Hong, *J. Chem. Soc., Dalton Trans.*, 2001, 2335; (*f*) S. A. Bourne, J. Lu, B. Moulton and M. J. Zaworotko, *Chem. Commun.*, 2001, 861.

19 (*a*) X.-J. Luan, X.-H. Cai, Y.-Y. Wang, D.-S. Li, C.-J. Wang, P. Liu, H.-M. Hu, Q.-Z. Shi and S.-M. Peng, *Chem.–Eur. J.*, 2006, **12**, 6281; (*b*) F. A. A. Paz and J. Klinowski, *Inorg. Chem.*, 2004, **43**, 3948; (*c*) J.-C. Dai, X.-T. Wu, Z.-Y. Fu, C.-P. Cui, S.-M. Hu, W.-X. Du, L.-M. Wu, H.-H. Zhang and R.-Q. Sun, *Inorg. Chem.*, 2002, **41**, 1391; (*d*) R. Wang, M. Hong, J. Luo, R. Cao and J. Weng, *Chem. Commun.*, 2003, 1018; (*e*) E. Suresh, K. Boopalan, R. V. Jasra and M. M. Bhadbhade, *Inorg. Chem.*, 2001, **40**, 4078; (*f*) R.-Q. Zou, X.-H. Bu and R.-H. Zhang, *Inorg. Chem.*, 2004, **43**, 5382.

20 (*a*) C.-L. Chen, A. M. Goforth, M. D. Smith, C.-Y. Su and H. C. zur Loye, *Inorg. Chem.*, 2005, **44**, 8762; (*b*) K.-J. Wei, Y.-S. Xie, J. Ni, M. Zhang and Q.-L. Liu, *Cryst. Growth Des.*, 2006, **6**, 1341.

21 (*a*) I. Persson and K. B. Nilsson, *Inorg. Chem.*, 2006, **45**, 7428; (*b*) A.-J. Zhou, S.-L. Zheng, Y. Fang and M.-L. Tong, *Inorg. Chem.*, 2005, **44**, 4475; (*c*) C. K. Tan, J. Wang, J.-D. Leng, L.-L. Zheng and M.-L. Tong, *Eur. J. Inorg. Chem.*, 2008, 771.

22 S. Reinoso, P. Vitoria, J. M. Gutiérrez-Zorrilla, L. Lezama, L. S. Felices and J. I. Beitia, *Inorg. Chem.*, 2005, **44**, 9731.

23 (*a*) J. E. McGarrah, Y.-J. Kim, M. Hissler and R. Eisenberg, *Inorg. Chem.*, 2001, **40**, 4510; (*b*) Q. Wu, M. Esteghamatian, N.-X. Hu, Z. Popovic, G. Enright, Y. Tao, M. D'Iorio and S. Wang, *Chem. Mater.*, 2000, **12**, 79; (*c*) G. D. Santis, L. Fabbrizzi, M. Licchelli, A. Poggi and A. Taglietti, *Angew. Chem., Int. Ed. Engl.*, 1996, **35**, 202.

24 (*a*) S. Dong, X. Xi and M. Tian, *J. Electroanal. Chem.*, 1995, **385**, 227; (*b*) B. Keita, A. Belhouari, L. Nadjo and R. Contant, *J. Electroanal. Chem.*, 1995, **381**, 243; (*c*) J. E. Toth and F. C. Anson, *J. Electroanal. Chem.*, 1988, **256**, 361.